On-demand all-optical generation of controlled Rb-vapor densities in photonic-band-gap fibers

Amar R. Bhagwat,* Aaron D. Slepkov, Vivek Venkataraman, Pablo Londero, and Alexander L. Gaeta
School of Applied and Engineering Physics, Cornell University, Ithaca, New York 14853, USA
(Received 13 February 2009; published 5 June 2009)

We investigate the time dynamics of light-induced desorption of Rb atoms in hollow-core photonic-band-gap fibers and demonstrate all-optical generation of precisely controlled Rb-vapor densities. We also compare the performance of the desorption process in an unmodified fiber with one with an organosilane-coated core, and based on the vapor depletion and recovery behavior, we propose a mechanism to describe the desorption processes. We further demonstrate that high densities of Rb vapor can be generated after the desorption beam is switched off and use it to realize Λ-scheme electromagnetically induced transparency at control powers as low as 80 nW.

DOI: 10.1103/PhysRevA.79.063809 PACS number(s): 42.65.Wi, 34.35.+a, 42.50.Gy, 42.70.Qs

I. INTRODUCTION

Low-light-level nonlinear optics [1] is key for many applications such as single-photon all-optical switches [2] and quantum nondemolition measurements of single photons [3]. Such strong nonlinear interactions require the following: (1) a large optical depth (OD) $\kappa=N\sigma L$, where N is the number density of atoms or molecules of the medium, σ is the absorption cross section of the medium, and L is the interaction length; and (2) a tightly confined light mode resulting in relatively high intensities at ultralow powers. Waveguide geometries provide long interaction lengths and tightly confined light modes making them highly suitable for performing such interactions, and by careful choice of the waveguide medium one can attain a very large absorption cross section σ.

Hollow-core photonic-band-gap fibers [4,5] are optical fibers with a hollow core surrounded by a honeycomblike photonic crystal structure. They offer low-loss light guidance over long lengths while maintaining a small effective mode area. Since most of the light is contained in the hollow core, the fiber contributes negligible nonlinearity to the light mode [6] and a nonlinear medium of choice may be injected into the hollow core [7–11]. This geometry is advantageous in allowing us to choose a strongly nonlinear medium that can yield low-light-level nonlinearities, or it can be used to enhance the response of weakly nonlinear materials and make it possible to perform nonlinear optics with them at moderate light powers.

We have previously used this geometry for demonstrating coherent atom-photon interactions with Rb vapor at ultralow-light control powers [12]. The fiber walls were coated with a self-assembled monolayer of organosilanes [n-octadecyl dimethyl methoxysilane (ODMS)] in order to prevent the Rb atoms from reacting with the walls and to reduce the effects of spin decoherence from collisions with the wall [13,14]. The technique of light-induced atomic desorption (LIAD) [15–17] was then used to generate a large population of Rb atoms inside the hollow core. Although this technique has made waveguide-based low-light-level nonlinear optics possible, further improvements are necessary to make the system practical. The desorption process is unfortunately depletive and once the fiber is desorbed with a full-power desorption beam (>40 mW), the fiber requires 2–3 h for recovery which dictates the intervals between successive experiments. The organosilane coating does not appear to reduce spin decoherence appreciably as evidenced by the large linewidth of the demonstrated electromagnetically induced transparency (EIT) [12]. The reason for this may be that the coating thickness is only a single monolayer and hence may not be thick enough to shield the atoms from Casimir-type electromagnetic interactions with the walls. Finally, an increase in the rate at which experiments can be performed is highly desirable since a large number of experiments implies a higher signal-to-noise ratio for the nonlinear processes, which would make this system more practical to use.

Here, we study the time dynamics of light-induced atomic desorption in hollow-core photonic-band-gap fibers using a pulsed desorption scheme to investigate the viability of controlled high-repetition-rate generation of Rb vapor. We show that coating the fibers does not affect the desorption mechanism which, furthermore, shows two distinct time signatures. We also investigate the recovery of desorption in the fiber and propose a mechanism to explain the desorption process based on our observations. Lastly, we observe a Rb vapor which persists after switching off the desorption beam, which we further use to demonstrate Λ-scheme EIT.

II. EXPERIMENTAL SETUP

Two fibers (4.5 cm each) from the same spool (AIR-6–800, Crystal Fibre A/S) are placed inside a vacuum cell (Fig. 1). One fiber specimen is unmodified while the other fiber core is coated with a self-assembled monolayer of ODMS, as previously described [12]. The steel vacuum cell has glass windows on either side to facilitate the coupling of light in and out of the fibers. A source of Rb is attached to the assembly to generate an ambient vapor of Rb in the cell. The vapor achieves equilibrium with the source after the cell "ripens" and then diffuses down the fiber cores. Both fibers are exposed to identical conditions in the cell in order to compare the difference between the coated and uncoated fi-

*arb59@cornell.edu

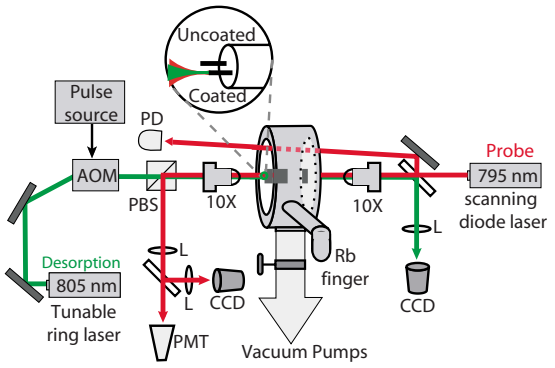

FIG. 1. (Color online) Two fibers: one coated and one uncoated (4.5 cm long) are placed inside a vacuum cell with glass windows on both sides. The desorption and probe lasers are coupled counterpropagating through a given fiber. A CCD camera is used to ascertain that the lasers are coupled to a single mode in the fiber core. A photodiode (PD) monitors the ambient Rb-vapor density in the cell. PMT: photomultiplier tube, L: lens, PBS: polarizing beam splitter, AOM: acousto-optic modulator.

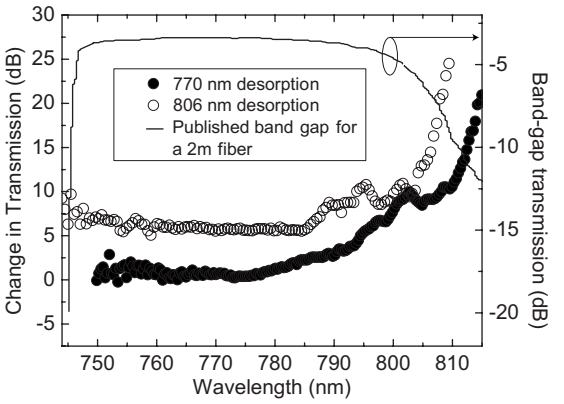

FIG. 2. Change in spectral transmission of a broadband probe beam due to the desorption process for a coated photonic-band-gap fiber over its entire band gap. The data represented by open circles are for a 806 nm desorption beam while those shown by the solid circles represent data for 770 nm desorption beam. The solid line shows the published band gap for a 2-m-long fiber and illustrates the band edges [20]. Both sets of data show a larger increase in transmission at the higher wavelength band edge. The data for an uncoated fiber follow similar trends (not shown).

bers with respect to their desorption performance. A weak probe beam (<1 nW, 795 nm) tuned to the ^{87}Rb D_1 transition ($F=1\rightarrow F'=2$) is coupled into the fiber to monitor the vapor generated inside the fiber. An 806 nm desorption beam (far detuned from any resonances) is coupled counterpropagating and cross-polarized to the probe beam for easier separation of the probe from any back-reflected desorption light incident on the detector. The power and duration of the desorption beam are controlled using an acousto-optic modulator (AOM) that varies the amount of power coupled into the fiber. Using the AOM we generate desorption pulses as short as 100 ns to study the desorption process at various time scales. The probe beam is passed through narrow-band 795 nm filters (TFI 795MC10) and is detected using a PMT (Hamamatsu H7422–50). The output of the PMT is coupled to an oscilloscope using a suitable impedance termination (Thorlabs VT1).

III. EFFECT OF DESORPTION ON FIBER TRANSMISSION

Before exposure to Rb, the coated fiber exhibits a lower transmission (10%–15%) than the uncoated one (25%–30%) at 795 nm. This indicates that the coating perturbs the band-gap guidance of the fiber possibly due to increased scattering from the coating, although the actual band gap is not seen to be altered significantly. The Rb atoms diffuse down the fiber core, are adsorbed on to the fiber walls, and diffuse transversely into the glass matrix facilitating further adsorption of Rb atoms on the surface. This ripening process of the fiber can be accelerated by desorbing regularly during the initial stages. We have observed that this adsorption process increases the scattering inside the fiber and reduces its light throughput and hence the fiber transmission. Exposing this fiber to a strong desorption beam not only desorbs the atoms but also increases the coupling of the desorption beam through the fiber. This generates a positive feedback wherein as the desorption beam coupling increases so does the rate of desorption, which increases the coupling further. For a fully ripened fiber, desorption can restore the transmission to 10% for a coated fiber and 20% for an uncoated fiber at 795 nm. Desorption from uncoated silica has been previously reported in specially prepared porous silica samples [18] and recently in hollow-core band-gap fibers [19]. Thus, organic coatings are not essential for light-induced desorption in silica.

The presence of adsorbed Rb atoms on the fiber walls changes the fiber transmission over its entire band gap. Figure 2 shows the ratio of transmission before and after desorption over the entire band gap for the coated fiber, which was probed using a broadband supercontinuum source. The increase in transmission is fairly uniform over the entire band gap except at the higher wavelength edge. The possibility of the formation of nanoclusters of adsorbed atoms on porous silica surfaces which exhibit resonances based on their sizes has been recently suggested [21]. In order to probe the possibility that nanoclusters resonant around 810 nm were selectively evaporated, we shifted the desorption wavelength to 770 nm to probe size-based resonances and selectively desorb 770 nm resonant nanoclusters that should result in an enhanced transmission at that wavelength. As shown in Fig. 2, the transmission change observed with 770 nm desorption beam is nearly identical to that with 806 nm. Size-based resonances having linewidths [22] greater than the fiber bandwidth cannot be distinguished clearly in the current setup, and it is possible that the fiber band gap is blue-detuned from the peak wavelength of surface-plasmon resonances of Rb nanoclusters formed inside the fiber core.

IV. TEMPORAL DYNAMICS OF LIAD

We characterize the temporal dynamics of the desorption process by coupling desorption pulses of varying duration

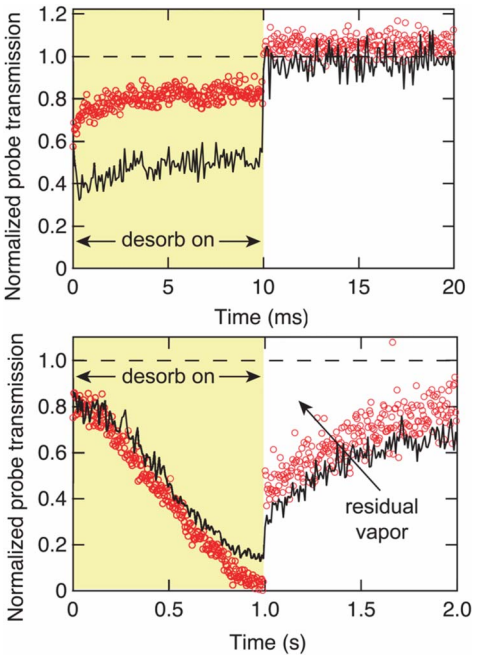

FIG. 3. (Color online) Desorption signature at two different time scales. The shaded area denotes the time for which desorption pulse is on, while the dashed line represents transmission in the absence of desorption. Data in red open circles indicate transmission change in a coated fiber while the data in uncoated fiber are indicated by the black solid line. The data have been corrected for fiber coupling changes due to desorption and only indicate the effect of Rb-vapor absorption. Relatively low desorption powers (10–15 mW incident) are used to generate optical depths suitable for displaying time dynamics with sufficient dynamic range.

into the fibers. During the desorption process the transmission of the fibers increases steadily over time. Hence, we use the off-resonance transmission of the probe to characterize the transmission increase, and normalize the on-resonance transmission data to it to obtain absorption information purely due to Rb vapor. When the fibers are exposed to 100 μs desorption pulses, immediately after turning on the desorption pulse, the Rb vapor increases within 10 μs and then slowly decays. Figure 3 shows the ratio of on- to off-resonance transmission indicating the absorption that is solely due to Rb vapor. For a 10 ms pulse [see Fig. 3(a)], we observe the transmission to decrease slightly and then remain constant over the entire duration of the pulse which indicates a steady generation of vapor. The time dynamics of coated and uncoated fibers are essentially identical and the coating may change the absolute amount of vapor produced but does not alter the dynamics of desorption. For a 1 s duration pulse, we observe that the OD remains steady for 50 ms after which a second desorption mechanism generates much higher vapor densities. This is manifested as a large decrease in on-resonance transmission despite the high off-resonance transmission (not shown), which indicates that Rb vapor is responsible for this absorption. As the absorption evolves further in time, we observe optical depths greater than 1000 in the fiber at longer time intervals [19]. After the desorption pulse is turned off, the off-resonance transmission is restored to its original value, but the on-resonance transmission remains low resulting in continued absorption [shown in Fig. 3(b)], which decreases slowly with time. We attribute the presence of this residual vapor to the fact that the amount of Rb population generated may be too high for complete immediate readsorption of the entire vapor. The fiber walls are saturated with adsorbed Rb atoms and the main adsorption rate is governed by diffusion through the glass. It has been reported that the diffusion of alkali-metal atoms through siloxane coatings can be modified by presence of light [16]. The limiting of adsorption rate in both coated and uncoated fibers suggests that fast light-induced diffusion of Rb out of the glass matrix and slow diffusion back into the glass could explain the behavior. The presence of residual vapor is advantageous for performing interactions with Rb vapor in the absence of any desorption beams, which can give rise to significant ac Stark shifts (>10 MHz/mW) and increased scattering resulting in perturbation of sensitive measurements. In fact, we have successfully used the residual vapor to demonstrate EIT as described below.

After exposure to a strong cw desorption beam, the fiber is completely depleted and requires approximately 2 h to recover before it can generate as much vapor as an undesorbed fiber. To understand how the fiber recovers and how the recovery depends on the ambient vapor pressure, the Rb source and the cell are cooled down to room temperature. A probe beam is passed directly through the cell to ensure that there is no measurable Rb vapor in the cell. Surprisingly, we observe that the fibers require the same amount of time to recover irrespective of the presence of ambient vapor, and the fibers continue to desorb for weeks (with regular desorptions every 2 h) after which they show a decrease in the generated Rb vapor. This shows that the Rb desorbed by the fiber is not in continuous equilibrium with the ambient vapor in the cell. Over a period of weeks, the atoms are lost either due to chemical means or through the fiber ends, which eventually results in a decrease in the generated vapor if no ambient vapor is present. Figure 4 shows the recovery of this desorption capacity over short time periods. The fiber is exposed to 1 ms desorption pulses carved out of a 40 mW beam and is probed by a weak cw beam tuned to an ^{87}Rb D_1 transition. Initially, an undepleted fiber is exposed to a single 1 ms desorption pulse to measure the original desorption capacity. The fiber is then exposed to a train of consecutive pulses (>30 at 50% duty cycle) till maximum depletion is achieved and the transmission is recorded. We then let the fiber recover in the dark and probe the density generated by a single 1 ms desorption pulse at different elapsed times. We observe both "fast" and "slow" mechanisms that produce a Rb vapor. As shown in Fig. 4, the fast mechanism produces a lower density of atoms, which peaks within a few μs and falls off. The slow mechanism produces a larger Rb density which slowly increases over a period of hundreds of μs and it is this mechanism which shows a distinct recovery as a function of time elapsed between depletion and probing. Unless the fiber is exposed to a strong continuous desorption (pulses longer than 100 ms), the recovery of the slow mechanism requires only 100 s as shown. When exposed to 100 ms or longer desorption pulses, we have observed that the slow mechanism takes tens of minutes to recover and fully recovers to its predesorption capacity after 2 h, which is consistent with our cw desorption results.

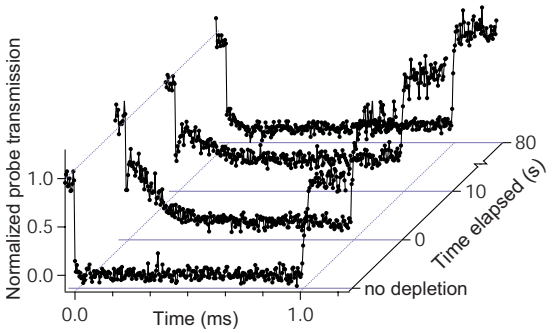

FIG. 4. (Color online) Recovery of desorption capacity of the uncoated fiber is studied. A 1 ms desorption pulse generates almost complete absorption of probe on the first exposure. After repeated exposure of the fiber to many 1 ms desorption pulses, the probe absorption at the beginning of the pulse shows depletion and is maximally depleted at elapsed time=0 s. The probe absorption is then recorded after exposure to identical 1 ms desorption pulses at subsequent time intervals, and we observe that the absorption slowly recovers to match its initial desorption capacity before depletion.

Based on the above observations, we present a model for the desorption mechanism in hollow-core fibers. We postulate that the Rb atoms can reside either (1) on the surface forming a contiguous metallic layer or noncontiguous agglomeration of nanoclusters or (2) diffused into the glass matrix. Over a period of time, the fiber can build up a significant reservoir of diffused Rb atoms within the fiber walls. When a desorption beam is coupled into the fiber, the wings of the transverse light mode interact with the surface Rb atoms and with the diffused atoms in the fiber walls. The fast desorption mechanism could then be a result of these surface atoms which undergo a relatively weak desorption due to photoinduced charge transfer from silica to Rb as discussed in [23]. The slower desorption mechanism possibly occurs due to resonant heating of nanoclusters due to size-based surface plasmon resonances [21] leading to the evaporation of the nanoclusters and resulting in a stronger desorption. The glass matrix may also play a role in sustaining the strong, slow desorption mechanism by acting as a reservoir of diffused atoms and replenishing atoms that may be lost over time from the surface. The possibility of two different sources of Rb atoms requiring different desorption and recovery times is corroborated by the desorption recovery data as shown in Fig. 4. Immediately after desorption, the atoms form a uniform coating on the core surface which is nonresonant with the probe and the fiber transmission remains high. Over a period of 2 h, the Rb population on the glass redistributes such that it agglomerates into nanoclusters that display enhanced scattering of coupled light over the entire band gap and can sustain another round of plasmon-resonance-based desorption.

V. INTENSITY DEPENDENCE OF DESORPTION

In order to generate a controlled OD by modulating the desorption beam, we calibrate the absorption as a function of desorption beam power at the input. It is important to note

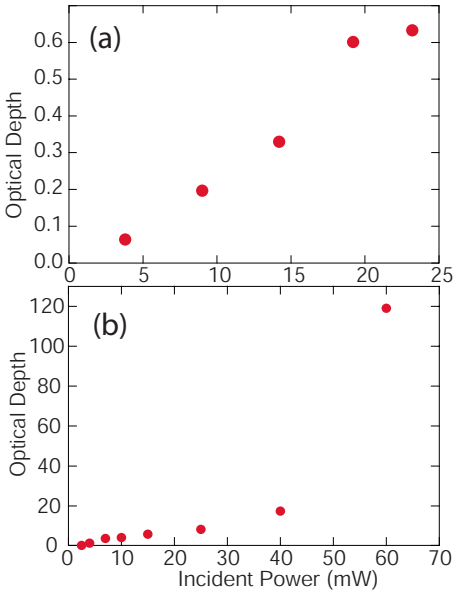

FIG. 5. (Color online) Optical depth generated as a function of incident desorption beam power in a coated fiber. (a) 50 μs pulses tuned on resonance are used to measure the absorption generated. The second, slower desorption mechanism does not contribute to this vapor generation. (b) Maximum steady OD generated by few-s long desorption pulses created by the second desorption mechanism.

that the OD varies over the duration of the desorption pulse, and we measure the OD generated by the fast mechanism when it stabilizes 50 μs after the desorption beam is switched on. In the case of the second, stronger mechanism, we measure the maximum OD produced by scanning across the entire D_1 Rb line during a few-s desorption pulse and extracting OD information by fitting with Voigt absorption profiles as described in [19]. In Fig. 5, OD is defined as optical depth as experienced by a light field on resonance on $^{85}\mathrm{Rb}(F=2\rightarrow F'=1,2)D_1$ transition.

Figure 5(a) shows that for short desorption pulses, the OD generated varies approximately linearly with incident power. OD measurement with short pulses at higher powers is not possible with this method because the vapor completely absorbs the probe and the precise OD cannot be measured. Figure 5(b) shows the high ODs generated by the second mechanism, where the trend is linear until 40 mW, at which point the OD exhibits a large increase in sensitivity to the power. This may be due to bulk heating generated in the fiber, which can give rise to a thermally generated Rb vapor.

By tailoring the intensity and duration of the pulses, controllable optical depths can be generated in a repeatable fashion as shown in Fig. 6(a). Generating vapor via the fast mechanism using short desorption pulses (<50 μs) has the additional advantage that the fiber is not completely depleted and can desorb continuously for hours while still producing the same amount of vapor from shot to shot. On the other hand, the residual vapor that persists after a strong desorption pulse (1 s or longer) is switched off can be used for low-light-level nonlinear optical experiments while avoiding the scatter from the desorption beam. We perform EIT in the Λ scheme in this residual vapor [see Fig. 6(b)]. The weak

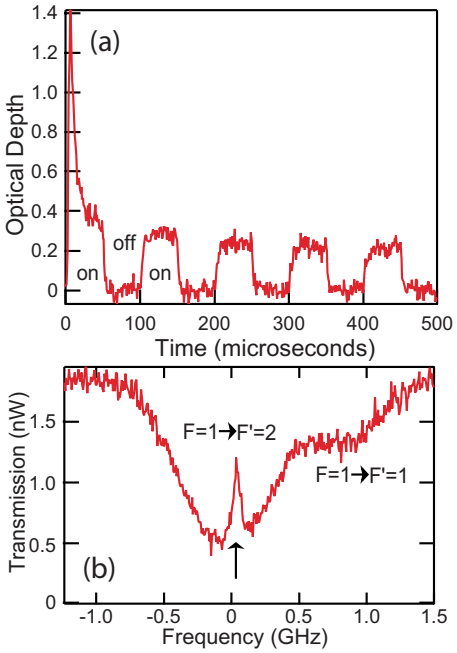

FIG. 6. (Color online) (a) Generation of controlled OD using 50 μs, 10 mW desorption pulses in a coated fiber. We see that the OD generated is uniform during the pulse and from pulse to pulse. The large peak in OD at the beginning likely corresponds to Rb atoms that undergo fast desorption but do not regenerate within 500 μs. (b) EIT in Λ scheme (shown by the arrow) demonstrated in the residual vapor generated in a coated fiber after a strong desorption pulse. The oscilloscope is triggered after the desorption beam is completely switched off. A very low control beam power (80 nW, tuned to $F=2\rightarrow F'=2$ transition) is used and the EIT peak shows no measurable light shift.

probe is scanned over the $(F=1\rightarrow F'=1,2)$ manifold of ^{87}Rb D_1 transition, while the control beam is coupled copropagating but cross-polarized to the probe beam and tuned to the $(F=2\rightarrow F'=2)$ transition of the D_1 line. Along with polarization isolation, we use an isotopically pure ^{85}Rb cell (broadened and shifted by 120 Torr N_2) to selectively absorb the control beam and separate it from the probe [24]. We achieve a significant EIT depth (50%) at 80 nW of pump power. The position of the EIT shows no light shifts as compared to when the desorption beam is on, thus demonstrating the advantage of using the residual vapor.

VI. SUMMARY

We have demonstrated on-demand and tunable Rb-vapor generation that can be operated without depleting the fiber significantly. Additionally, we have shown that this vapor can be accessed in the absence of any desorption beam in the form of the residual vapor and have demonstrated Λ-scheme EIT in the residual vapor. We propose that two mechanisms exist for desorption in hollow-core band-gap fibers by analyzing the time dynamics of desorption and the recovery data. The nonresonant atoms undergo a fast and weaker desorption, whereas the nanoclusters formed via redistribution of adsorbed atoms undergo a slower but stronger resonant desorption. We have also compared the effect of coating the fiber core on desorption and have not found significant difference in either the time dynamics or band-gap measurements. The ability to conduct nanowatt-light-level nonlinear optical processes in fibers using a nondepleting high repetition rate desorption scheme is a significant advancement toward hollow-waveguide-based nonlinear optical systems.

ACKNOWLEDGMENTS

The authors gratefully acknowledge financial support from the Center for Nanoscale Systems, the Air Force Office of Scientific Research, and DARPA under the Slow-Light program.

[1] S. E. Harris and L. V. Hau, Phys. Rev. Lett. **82**, 4611 (1999).
[2] S. E. Harris and Y. Yamamoto, Phys. Rev. Lett. **81**, 3611 (1998).
[3] H. Schmidt and A. Imamogdlu, Opt. Lett. **21**, 1936 (1996).
[4] R. F. Cregan, B. J. Mangan, J. C. Knight, T. A. Birks, P. S. J. Russell, P. J. Roberts, and D. C. Allan, Science **285**, 1537 (1999).
[5] P. S. Russell, J. Lightwave Technol. **24**, 4729 (2006).
[6] C. J. Hensley, D. G. Ouzounov, A. L. Gaeta, N. Venkataraman, M. T. Gallagher, and K. W. Koch, Opt. Express **15**, 3507 (2007).
[7] F. Benabid, J. C. Knight, G. Antonopoulos, and P. S. J. Russell, Science **298**, 399 (2002).
[8] D. G. Ouzounov, F. R. Ahmad, D. Muller, N. Venkataraman, M. T. Gallagher, M. G. Thomas, J. Silcox, K. W. Koch, and A. L. Gaeta, Science **301**, 1702 (2003).
[9] S. Ghosh, J. E. Sharping, D. G. Ouzounov, and A. L. Gaeta, Phys. Rev. Lett. **94**, 093902 (2005).
[10] P. S. Light, F. Benabid, F. Couny, M. Maric, and A. N. Luiten, Opt. Lett. **32**, 1323 (2007).
[11] A. R. Bhagwat and A. L. Gaeta, Opt. Express **16**, 5035 (2008).
[12] S. Ghosh, A. R. Bhagwat, C. K. Renshaw, S. Goh, A. L. Gaeta, and B. J. Kirby, Phys. Rev. Lett. **97**, 023603 (2006).
[13] J. C. Camparo, J. Chem. Phys. **86**, 1533 (1987).
[14] M. A. Bouchiat and J. Brossel, Phys. Rev. **147**, 41 (1966).
[15] A. Gozzini, F. Mango, J. H. Xu, G. Alzetta, F. Maccarrone, and R. A. Bernheim, Nuovo Cimento D **15**, 709 (1993).
[16] S. N. Atutov, V. Biancalana, P. Bicchi, C. Marinelli, E. Mariotti, M. Meucci, A. Nagel, K. A. Nasyrov, S. Rachini, and L. Moi, Phys. Rev. A **60**, 4693 (1999).
[17] E. B. Alexandrov, M. V. Balabas, D. Budker, D. English, D. F. Kimball, C.-H. Li, and V. V. Yashchuk, Phys. Rev. A **66**, 042903 (2002).
[18] A. Burchianti, C. Marinelli, A. Bogi, J. Brewer, K. Rubahn, H.-G. Rubahn, F. Della Valle, E. Mariotti, V. Biancalana, S. Veronesi, and L. Moi, Europhys. Lett. **67**, 983 (2004).
[19] A. D. Slepkov, A. R. Bhagwat, V. Venkataraman, P. Londero, and A. L. Gaeta, Opt. Express **16**, 18976 (2008).

[20] Air-6–800 fiber datasheet, http://www.crystal-fibre.com/datasheets/AIR-6-800.pdf
[21] A. Burchianti, A. Bogi, C. Marinelli, C. Maibohm, E. Mariotti, and L. Moi, Phys. Rev. Lett. **97**, 157404 (2006).
[22] A. Burchianti, A. Bogi, C. Marinelli, C. Maibohm, E. Mariotti, S. Sanguinetti, and L. Moi, Eur. Phys. J. D **49**, 201 (2008).
[23] B. V. Yakshinskiy and T. E. Madey, Nature (London) **400**, 642 (1999).
[24] N. Kuramochi, I. Matsuda, and H. Fukuyo, J. Opt. Soc. Am. **68**, 1087 (1978).